ORIGINAL ARTICLE

Cancer Science WILEY

Component with abundant immune-related cells in combined hepatocellular cholangiocarcinoma identified by cluster analysis

Naoki Yagi[1,2,3] | Toshihiro Suzuki[1,4] | Shoichi Mizuno[1] | Motohiro Kojima[5] |
Masashi Kudo[2] | Motokazu Sugimoto[2] | Shin Kobayashi[2] | Naoto Gotohda[2,3] |
Genichiro Ishii[3,6] | Tetsuya Nakatsura[1]

[1]Division of Cancer Immunotherapy, Exploratory Oncology Research and Clinical Trial Center, National Cancer Center, Kashiwa, Japan

[2]Department of Hepatobiliary and Pancreatic Surgery, National Cancer Center Hospital East, Kashiwa, Japan

[3]Course of Advanced Clinical Research of Cancer, Juntendo University Graduate School of Medicine, Tokyo, Japan

[4]Department of Pharmacology, School of Medicine, Teikyo University, Tokyo, Japan

[5]Division of Pathology, Exploratory Oncology Research and Clinical Trial Center, National Cancer Center, Kashiwa, Japan

[6]Department of Pathology and Clinical Laboratories, National Cancer Center Hospital East, Kashiwa, Japan

Correspondence
Tetsuya Nakatsura, Division of Cancer Immunotherapy, Exploratory Oncology Research and Clinical Trial Center, National Cancer Center, Kashiwa, Japan.
Email: tnakatsu@east.ncc.go.jp

Abstract

Combined hepatocellular cholangiocarcinoma (cHCC-CCA) is a heterogeneous tumor sharing histological features with hepatocellular carcinoma (HCC) and intrahepatic cholangiocarcinoma (iCCA). The tumor immune microenvironment (TIME) of cHCC-CCA is unclear. We compared the TIME of cHCC-CCA with that of HCC and iCCA. Twenty-three patients with cHCC-CCA after hepatectomy were evaluated in this study. Twenty-three patients with iCCA and HCC were also included. iCCA was matched for size, and HCC was matched for size and hepatitis virus infection with cHCC-CCA. Immune-related cells among the iCCA-component of cHCC-CCA (C-com), HCC-component of cHCC-CCA (H-com), iCCA, and HCC were assessed using multiplex fluorescence immunohistochemistry. Among C-com, H-com, iCCA, and HCC, multiple comparisons and cluster analysis with k-nearest neighbor algorithms were performed using immunological variables. Although HCC had more T lymphocytes and lower PD-L1 expression than iCCA ($P < 0.05$), there were no significant differences in immunological variables between C-com and H-com. C-com tended to have more T lymphocytes than iCCA ($P = 0.09$), and C-com and H-com had fewer macrophages than HCC ($P < 0.05$). In cluster analysis, all samples were classified into two clusters: one cluster had more immune-related cells than the other, and 12 of 23 H-com and eight of 23 C-com were identified in this cluster. The TIME of C-com and H-com may be similar, and some immunological features in these components were different from those in HCC and some iCCA. Cluster analysis identified components with abundant immune-related cells in cHCC-iCCA.

KEYWORDS
cluster analysis, hepatocellular carcinoma, hepatocellular cholangiocarcinoma, immunohistochemistry, tumor microenvironment

1 | INTRODUCTION

Combined hepatocellular cholangiocarcinoma (cHCC-CCA) is a rare tumor characterized by hepatocellular and glandular features. The incidence of cHCC-CCA has been reported as 0.7%–14.2% among patients with primary liver cancer.[1-3] The prognosis of cHCC-CCA is better than that of intrahepatic cholangiocarcinoma (iCCA) but poorer than that of hepatocellular carcinoma (HCC),[4] and surgical resection is the only treatment for cHCC-CCA. However, there is no consensus regarding systemic treatments for patients with unresectable cHCC-CCA, and these treatments are often selected from among those intended for patients with HCC or iCCA.[5-7] Recently, immunotherapies, including immunocheckpoint inhibitors, have emerged as alternative treatments for patients with advanced solid tumors.[8] In Japan, the combination of atezolizumab and bevacizumab has replaced sorafenib as the first-line treatment for unresectable HCC.[9,10] Moreover, peptide vaccine therapy[11,12] and adoptive cell transfer[13,14] have been reported to be effective against HCC. Contrastingly, for iCCA, immunotherapy has resulted in antitumor responses, but only in a select group of patients; consequently, the introduction of suitable indications has been delayed.[15,16] However, patients with cHCC-CCA are mostly excluded from clinical trials on immunotherapies because of the rarity and specific features of this disease[6]; there is only one case report on using immune therapy for treating cHCC-CCA.[17]

Interpretation of the tumor immune microenvironment (TIME) is important for exploring the therapeutic indication of immunotherapy.[18] Recent studies have shown that high expression of PD-L1[19,20] and abundant tumor-infiltrating lymphocytes[21-23] are correlated with the treatment effectiveness of immunotherapy. In the present study, we investigate the composition of TIME in cHCC-iCCA via comparisons and clustering analyses in two contrasting tumors: HCC, a carcinoma that has been shown to respond suitably to immunotherapy, and iCCA, a carcinoma that responds poorly to immunotherapy. The results of the present study could facilitate the introduction of suitable immunotherapies for the disease in future.

2 | MATERIAL AND METHODS

2.1 | Patients

Twenty-three patients who underwent hepatectomy and were diagnosed with cHCC-CCA between June 2003 and June 2018 at the National Cancer Center Hospital East (Chiba, Japan) were investigated in this study. Using a one-to-one matching approach, 23 size-matched patients from among 55 patients who underwent hepatectomy and were diagnosed with iCCA were also investigated; we also randomly included 23 size- and hepatitis virus infection-matched patients from among 396 patients who underwent hepatectomy and were diagnosed with HCC between January 2009 and June 2018 at the National Cancer Center Hospital East. The clinico-pathological variables of the 69 patients are listed in Table S1.

2.2 | Discrimination between iCCA and HCC component of cHCC-CCA via H&E staining

Formalin-fixed paraffin-embedded tumor tissues were sectioned into 4-μm thick serial sections for each patient with cHCC-CCA, HCC, and iCCA. The sections were subjected to H&E staining. The iCCA-like component and HCC-like component were defined as described previously,[4] i.e., the iCCA component (C-com) was defined as "an area characterized by glandular differentiation with mucin production and abundant fibrous stroma" and the HCC component (H-com) was defined as "an area characterized by trabecular growth with bile production, abundant eosinophilic cytoplasm, and prominent nucleoli." For the mixed subtype, H-com and C-com were defined as areas where an HCC and iCCA area accounted for more than 90%, respectively. Intermediate regions were excluded from evaluation. Each component was differentiated under the supervision of an experienced pathologist (M.K.) for all patients with cHCC-CCA.

Figure S1 shows an example of the differentiation procedure for each component via H&E staining of the cHCC-CCA tissues.

2.3 | Multiplex fluorescence immunohistochemistry

Immunohistochemistry was performed on 4-μm thick tissue sections of cHCC-CCA, iCCA, and HCC. The sections were subjected to multiplex fluorescence immunohistochemistry (MFIH) using a PerkinElmer Opal Kit. Two patterns of MFIH combined with various antibodies were prepared. Table S2 lists the primary antibody conditions used for staining. MFIH images were acquired using an automated multisector imaging system (Vectra version 3.0; PerkinElmer). Figure 1 shows illustrative MFIH images of cHCC-CCA specimens. A maximum of 20 regions of interest (ROIs) (699 × 500 μm) were randomly selected from the C-com and H-com, which were discriminated using H&E staining of the cHCC-CCA specimens (Figure S2). Twenty ROIs (699 × 500 μm) were randomly selected for HCC and iCCA.

2.4 | Histological and immunological evaluation

Table S3 presents the features of the areas evaluated in cHCC-CCA, iCCA, and HCC samples. An image analysis program (Inform 2.4; PerkinElmer) was used to evaluate the ROI of each tumor, stroma, and nonevaluated tissue, such as the intraluminal structures, as well as to detect immune-related cells with specific phenotypes; the distribution of immune-related cells was analyzed. Figure S3 illustrates the trainable tissue segmentation in cHCC-CCA. Training sessions for tissue segmentation and phenotype recognition were performed repeatedly until the algorithm attained the level of confidence recommended by the manufacturer (at least 90% accuracy).[24,25] Numerical data of tissues and immune-related cells calculated from
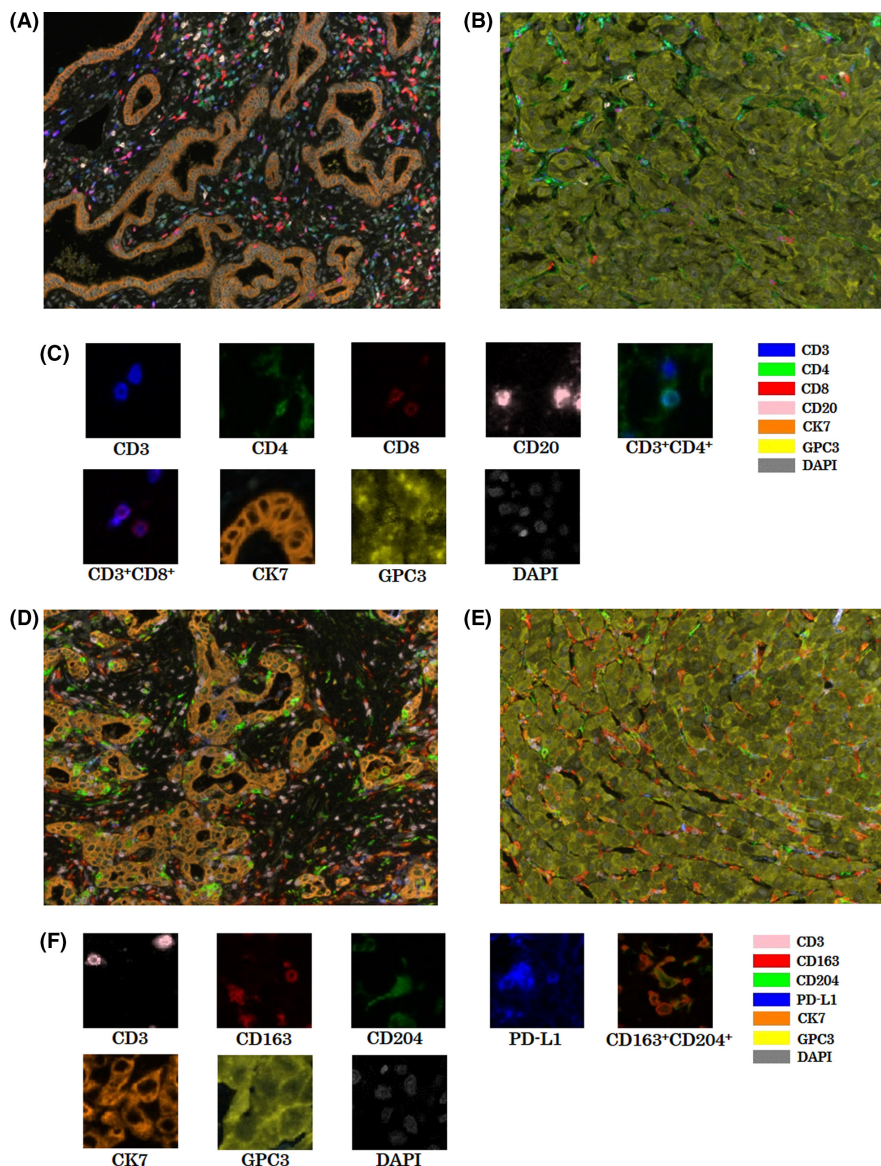
FIGURE 1 Example images of multiplex fluorescence immunohistochemistry (MFIH) for combined hepatocellular cholangiocarcinoma (cHCC-CCA). We used nine types of primary antibodies and combined them to establish two types of MFIH patterns. One pattern of MFIH was composed of anti-cluster of differentiation 3 (CD3), anti-cluster of differentiation 4 (CD4), anti-cluster of differentiation 8 (CD8), anti-cluster of differentiation 20 (CD20), anti-cytokeratin 7 (CK7) , anti-glypican-3 (GPC3), and 4′,6-diamidino-2-phenylindole (DAPI). The other pattern included anti-CD3, anti-CD4, anti-cluster of differentiation 163 (CD163), anti-cluster of differentiation 204 (CD204), anti- programmed cell death ligand 1 (PD-L1), anti-CK7, anti-GPC3, and DAPI. (A–C) One pattern of MFIH; (D–F) the other pattern. (A) intrahepatic cholangiocarcinoma component of cHCC-CCA (C-com). (B) hepatocellular carcinoma component of cHCC-CCA (H-com). (C) Magnified images of each antibody staining; opal 520 nm for anti-CK7 antibody, opal 540 nm for anti-CD3, opal 570 nm for anti-CD8, opal 620 nm for anti-CD4, opal 650 nm for anti-CD20, and opal 690 nm for anti-GPC3. (D) C-com of cHCC-CCA. (E) H-com of cHCC-CCA. (F) Magnified images of each antibody staining; opal 520 nm for anti-CK7, opal 540 nm for anti-CD3, opal 570 nm for anti-CD163, opal 620 nm for anti-CD204, opal 650 nm for anti-PD-L1, and opal 690 nm for anti-GPC3

Inform were analyzed using visual data analysis software (TIBCO Spotfire Analyst 7.11.1; TIBCO Software, Inc.). Cells in the whole tissue were defined as the sum of cells in the areas of tumor tissue and stroma tissue. Cell density was calculated as the number of cells per square millimeter, and the average value for each ROI was defined as the cell density for each sample. In addition, histological and immunological variables were analyzed for each C-com and H-com in cHCC-CCA. Histological evaluation was performed based on the area proportion of the tumor tissue, area proportion of the stroma tissue, cytokeratin 7 (CK7) positivity, and glypican-3 (GPC3) positivity. Immunological evaluation was performed based on the presence of CD3$^+$, CD3$^+$CD4$^+$, CD3$^+$CD8$^+$, CD20$^+$, and CD163$^+$CD204$^+$ cells in each tumor, stroma, and whole tissue, and the area characterized by PD-L1 positivity. We defined high PD-L1 expression among CD163$^+$CD204$^+$ cells using the gating strategy provided in TIBCO Spotfire Analyst 7.11.1.

2.5 | Cluster analysis with immunological variables

Cluster analysis with immunological variables from MFIH was performed using the *k*-nearest neighbor (*k*-NN) parameter calculated using *Seurat* version 4.0 package in the R version 4.1.0 environment (R Project for Statistical Computing). Multiple immunological features used as immunological variables are presented in Table S4.

2.6 | Statistical analysis

Continuous variables are presented as medians and ranges, whereas categorical variables are presented as numbers and percentages. The significance of continuous and categorical variables between the two groups was evaluated using the Wilcoxon test and Pearson's chi-square test, respectively. Multiple comparisons were performed using the Steel–Dwass test. These statistics tests were performed using JMP version 16.0.0 (SAS Institute, Inc.). Heat maps and dendrograms with hierarchical clustering based on Ward's method were created using JMP version 16.0.0. A scatter plot was drawn using *t*-distributed stochastic neighbor embedding (*t*-SNE) for continuous variables. The *t*-SNE, heat map, and violin plots were generated using the *Seurat* version 4.0 package in the R version 4.1.0 environment. Analysis items with $P < 0.05$ were significant.

3 | RESULTS

3.1 | Comparison of histological variables

Table 1 shows the comparison of histological variables between iCCA and HCC. The area proportion of the stroma tissue (20.6% vs. 5.9%, $P < 0.001$) and CK7 positivity (90.1% vs. 0.2%, $P < 0.001$) was higher, and that of the tumor (78.8% vs. 93.9%, $P = 0.002$) and GPC3 positivity (5.2% vs. 92.1%, $P < 0.001$) was lower in iCCA than in HCC. Table 2 shows a comparison of the histological variables between C-com and H-com. C-com exhibited a higher area proportion of the stroma tissue (41.2% vs. 13.7%, $P < 0.001$) and CK7 positivity (75.6% vs. 18.1%, $P = 0.038$), and a lower area proportion of the tumor tissue (55.9% vs. 86.3%, $P < 0.001$) and GPC3 positivity (4.9% vs. 40.7%, $P = 0.005$) compared to H-com.

3.2 | Comparison of immunological variables

Tables 3 and S4 show multiple comparisons of immunological variables among iCCA, HCC, C-com, and H-com. Compared with those in HCC, the densities of almost all immune-related cells in the tumor tissue of iCCA were lower; $CD3^+$ (22.8/mm^2 vs. 75.2/mm^2, $P = 0.047$), $CD3^+CD4^+$ (10.8/mm^2 vs. 37.7/mm^2, $P = 0.018$), and $CD163^+CD204^+$ (157.5/mm^2 vs. 545.2/mm^2, $P < 0.001$), excluding $CD3^+CD8^+$ (11.3/mm^2 vs. 33.3/mm^2, $P = 0.112$) and $CD20^+$ (18.1/mm^2 vs. 27.1/mm^2,

TABLE 1 Comparison of histological variables between iCCA and HCC

Variables	iCCA n = 23	HCC n = 23	P value iCCA vs. HCC
Area proportion			
Stroma tissue, %, median, [range]	20.6 [3.8–34.4]	5.9 [0–41.2]	<0.001
Tumor tissue, %, median, [range]	78.8 [68.8–96.2]	93.9 [58.8–100]	0.002
Area positive for multiple fluorescent immunostaining			
CK7, %, median, [range]	90.1 [56.4–98.3]	0.2 [0–71.0]	<0.001
GPC3, %, median, [range]	5.2 [0–21.4]	92.1 [11.2–99.9]	<0.001

Abbreviations: CK7, cytokeratin-7; GPC3, glypican-3; HCC, hepatocellular carcinoma; iCCA, intrahepatic cholangiocarcinoma.

TABLE 2 Comparison of histological variables between C-com and H-com

Variables	C-com n = 23	H-com n = 23	P value C-com vs. H-com
Area proportion			
Stroma tissue, %, median, [range]	41.2 [10.1–65.6]	13.7 [2.9–78.8]	<0.001
Tumor tissue, %, median, [range]	55.9 [34.4–89.4]	86.3 [21.2–97.1]	<0.001
Area positive for multiple fluorescent immunostaining			
CK7, %, median, [range]	75.6 [0.3–99.9]	18.1 [0–99.0]	0.038
GPC3, %, median, [range]	4.9 [0–59.4]	40.7 [0.6–91.9]	0.005

Abbreviations: C-com, iCCA component of combined hepatocellular-cholangiocarcinoma; CK7, cytokeratin-7; GPC3, glypican-3; H-com, HCC component of combined hepatocellular-cholangiocarcinoma.

TABLE 3 Multiple comparison of immune-related cells in the tumor tissue among iCCA, HCC, C-com, and H-com

Variables	iCCA	HCC	C-com	H-com	p-value					
	$n = 23$	$n = 23$	$n = 23$	$n = 23$	iCCA vs. HCC	iCCA vs. C-com	C-com vs. H-com	iCCA vs. H-com	HCC vs. C-com	HCC vs. H-com
CD3$^+$ cells/mm^2, median [range]	22.8 [2.3–330.6]	75.2 [6.4–735.4]	44.6 [3.4–731.7]	46.7 [3.1–336.2]	0.047	0.087	0.988	0.205	0.953	0.972
CD3$^+$CD4$^+$ cells/mm^2, median [range]	10.8 [0.4–177.4]	37.7 [2.2–343.9]	18 [1.5–314.7]	18.8 [2.5–305.7]	0.018	0.237	0.998	0.2223	0.838	0.859
CD3$^+$CD8$^+$ cells/mm^2, median [range]	11.3 [0.7–204.5]	33.3 [3.8–585.4]	30.3 [1.9–417.0]	23.5 [0.5–153.6]	0.112	0.107	0.934	0.252	1.000	0.887
CD20$^+$ cells/mm^2, median [range]	18.1 [0.7–297.5]	27.1 [2.2–271.4]	20.86 [0–211.8]	22.4 [0–184.5]	0.990	0.976	1.000	0.985	1.000	1.000
CD163$^+$CD204$^+$ cells/mm^2, median [range]	157.5 [40.7–587.4]	545.2 [126.9–930.0]	144.5 [13.8–1483.7]	241.7 [13.4–858.0]	<0.001	1.000	0.838	0.649	0.009	0.024
PD-L1 positivity %, median [range]	24.3 [1.4–62.9]	4.4 [0–56.8]	7.6 [0.7–94.5]	8.8 [0.5–80.6]	0.003	0.594	0.988	0.273	0.262	0.441
PD-L1 high cell in CD163$^+$CD204$^+$ %, median [range]	9.0 [0.6–63.4]	4.6 [0–87.5]	3.6 [0–75.6]	4.8 [0–61.1]	0.328	0.383	1.000	0.415	0.997	1.000

Abbreviations: C-com, iCCA component of combined hepatocellular cholangiocarcinoma; H-com, HCC component of combined hepatocellular cholangiocarcinoma; HCC, hepatocellular carcinoma; iCCA, intrahepatic cholangiocarcinoma; PD-L1, programmed cell death ligand 1.

$P = 0.990$). The proportion of the area characterized by PD-L1 positivity (24.3% vs. 4.4%, $P = 0.003$) was higher in iCCA than that in HCC.

The density of CD3$^+$ cells in the tumor tissue of C-com tended to be higher than that in iCCA (C-com vs. iCCA, 22.8/mm^2 vs. 44.6/mm^2, $P = 0.087$). The density of CD163$^+$CD204$^+$ cells in the tumor tissue of both C-com and H-com was lower than that in HCC (C-com vs. HCC, 144.5/mm^2 vs. 545.2/mm^2, $P = 0.009$; H-com vs. HCC, 241.7/mm^2 vs. 545.2/mm^2, $P = 0.024$). C-com and H-com showed no significant differences.

Based on the immunological variables of C-com, the distribution of each patient is shown on the heat map associated with dendrograms by hierarchical clustering based on Ward's method (Figure 2). Although some cases exhibited differences in immunological features between C-com and H-com, almost all cases showed similar trends in immunological features between these components. HCC cases tended to have more immune-related cells than iCCA, C-com, and H-com tissues. In contrast, some iCCA cases showed fewer lymphocytes compared to in C-com and H-com tissue.

3.3 | Visualization of immunological variables among iCCA, HCC, C-com, and H-com using t-SNE plots

Figure 3 shows the t-SNE plots of immunological variables among iCCA, HCC, C-com, and H-com (Figure 3A). HCC was distributed separately from iCCA. C-com and H-com were distributed randomly. In cluster analysis using the k-NN parameter, all samples were categorized into two clusters, clusters 0 and 1 (Figure 3B). Table 4 shows a comparison of immunological variables in clusters 0 and 1. Cluster 0 contained more infiltrating immune-related cells in all evaluated areas of the whole tissue, stroma tissue, and tumor tissue than those in cluster 1, and the proportion of the area characterized by PD-L1 positivity was higher in cluster 0 (12.5% vs. 7.6%, $P < 0.040$). Heat maps and violin plots of immunological variables in clusters 0 and 1 are shown in Figures 4 and S4, respectively.

The t-SNE plot of each group is shown in Figure 3C. HCC was identified more frequently in cluster 0 compared to iCCA (82.6% vs. 34.8%, $P = 0.001$). Twelve of the 23 H-com and eight of 23 C-com were identified in cluster 0; no significant difference was observed in the distribution between H-com and C-com (H-com vs. C-com, 52.2% vs. 34.8%, $P = 0.234$). Thirteen of the 23 cHCC-CCA (56.5%) were identified as cluster 0 in C-com and/or H-Com, and seven (30.4%) were identified as cluster 0 in both C-com and H-com. Cases with cluster 0 in C-com had more cases in which H-com was identified as cluster 0 than cases with cluster 1 in C-com (cluster 0 vs. cluster 1, 87.5% vs. 12.5%, $P = 0.013$).

4 | DISCUSSION

cHCC-CCA is a heterogeneous tumor that was first reported in 1903[26] and is diagnosed through routine histopathology based on
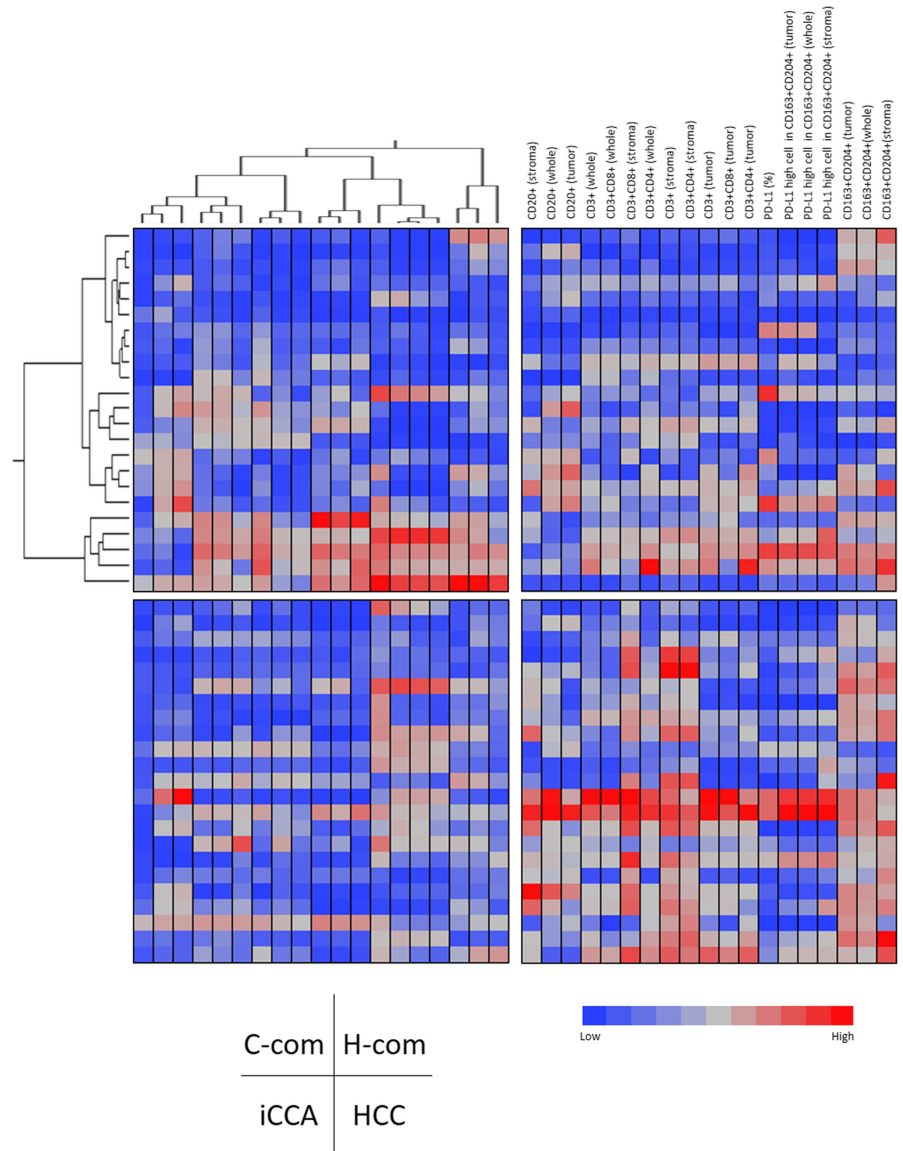
H&E staining with immunohistochemistry used as an adjunct.[6,27] Our previous study showed that GPC3 and CK7 are pathological markers for H-com and C-com, respectively.[28–30] In this study, we also defined the tissue components of cHCC-CCA as C-com and H-com, and then compared the various tissue features of these components. As expected, C-com and H-com exhibited histological characteristics and immunohistochemistry findings similar to those of iCCA and HCC, respectively (Tables 1 and 2).

Next, we evaluated the TIME of C-com, H-com, HCC, and iCCA through multiple comparison analysis (Tables 3 and S4). HCC had more CD3^{+} cells and lower PD-L1 expression compared to iCCA in the tumor tissue, suggesting that the TIME is more active in HCC than in iCCA. We speculated that these results may be related to the fact that immunotherapy against iCCA is not as effective against HCC. In cHCC-iCCA, although some patients showed different immunological features between each component, we observed no significant differences in immunological features between H-com and C-com (Tables 3 and S4, and Figure 2). A previous report suggested that

H-com and C-com in cHCC-CCA have different immune microenvironments, with more CD3^{+} and CD8^{+} cells observed in H-com than in C-com.[31] The differences between our results and the previous report may be related to the small number of cases, the fact that as many as 82.6% of cases were a mixed type, and the analysis of statistical significance using multiple comparison tests. These results suggest that the infiltration of immune cells is related to some intrinsic features of cHCC-CCA, including tumor antigenicity, rather than the histological characteristics of the tumor tissue. In the comparison of HCC, C-com, and H-com, the density of CD163^{+}CD204^{+} cells, known as tumor-associated macrophages (TAMs) of the immunosuppressive cells,[32,33] was lower in C-com and H-com than in HCC (Tables 3 and S4). In the comparison of iCCA, C-com, and H-com, C-com tended to have more CD3^{+} cells than iCCA. Moreover, some cases in C-com and H-com had more lymphocytes than in iCCA. Thus, C-com and H-com may have distinct TIME in both HCC and iCCA.

Visualization of the immunological features of the TIME in each case revealed that the distribution of iCCA greatly differed from that
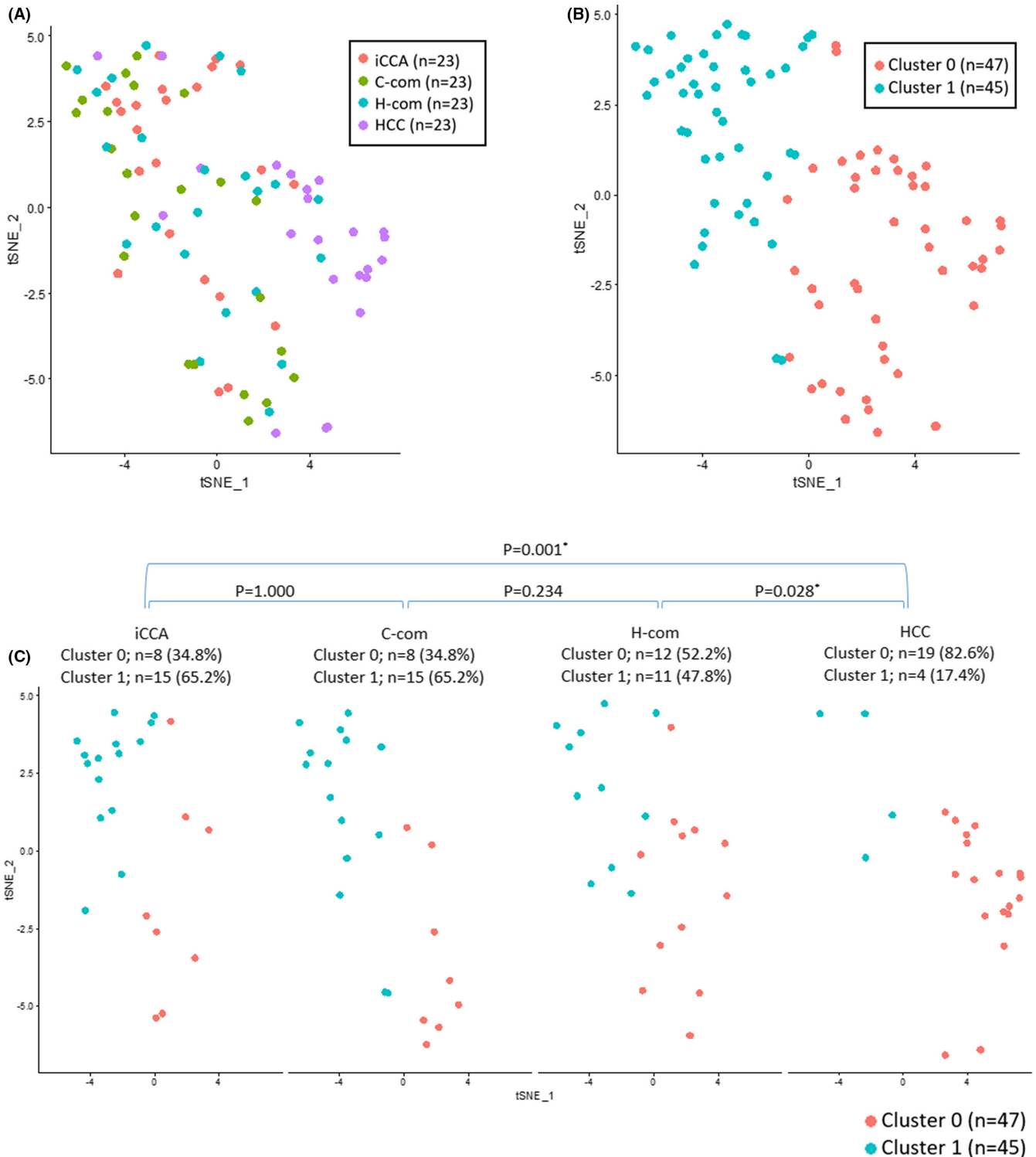
FIGURE 3 Scatter plot created from *t*-distributed stochastic neighbor embedding (*t*-SNE) of immunological variables among intrahepatic cholangiocarcinoma (iCCA), hepatocellular carcinoma (HCC), iCCA component of combined hepatocellular cholangiocarcinoma (cHCC-CCA) (C-com), and HCC component of cHCC-CCA (H-com). (A) Scatter plot using *t*-SNE and clustering using immune features. iCCA, HCC, C-com, and H-com are color-coded by group. (B) Clustering using the *k*-nearest neighbor parameter and searching for a common cluster. (C) iCCA, HCC, C-com, and H-com were defined as two groups: cluster 0 (*n* = 47) and cluster 1 (*n* = 45). *t*-SNE plot of each group

of HCC. In contrast, C-com and H-com were distributed randomly (Figure 3A). We cross-sectionally evaluated the immune microenvironment of C-com, H-com, HCC, and iCCA via cluster analysis of all patients and identified two clusters, cluster 0 and 1, based on the

immunological features (Figure 3B,C). Moreover, some patients with cHCC-CCA belonging to cluster 0 showed more active infiltration of lymphocytes. The concept of hot and cold tumors has become widely accepted in the field of immuno-oncology. Hot tumors are

TABLE 4 Comparison of immunological variables between patients in cluster 0 and cluster 1

Variables	Cluster 0 $n = 47$	Cluster 1 $n = 45$	P value
CD3$^+$			
Whole, cells/mm^2, median [range]	228.5 [33.7–1629.5]	85.9 [20.1–514.8]	<0.001
Stroma, cells/mm^2, median [range]	1174.6 [114.7–4954.9]	339.3 [71.6–1114.7]	<0.001
Tumor, cells/mm^2, median [range]	101.9 [2.3–735.4]	22.8 [2.5–199.0]	<0.001
CD3$^+$CD4$^+$			
Whole, cells/mm^2, median [range]	104.0 [10.1–646.6]	38.2 [5.8–235.1]	<0.001
Stroma, cells/mm^2, median [range]	591.7 [44.6–3535.9]	157.7 [12.4–621.6]	<0.001
Tumor, cells/mm^2, median [range]	46.8 [1.6–343.9]	8.9 [0.4–67.8]	<0.001
CD3$^+$CD8$^+$			
Whole, cells/mm^2, median [range]	115.5 [13.7–1162.2]	42.8 [12.6–279.6]	<0.001
Stroma, cells/mm^2, median [range]	541.9 [47.2–1974.3]	175.5 [38.8–520.5]	<0.001
Tumor, cells/mm^2, median [range]	54.8 [0.7–585.4]	9.4 [0.5–131.2]	<0.001
CD20$^+$			
Whole, cells/mm^2, median [range]	40.8 [2.5–494.4]	24.4 [0.2–261.3]	0.040
Stroma, cells/mm^2, median [range]	120.0 [0–2196.9]	27.7 [0–322.1]	<0.001
Tumor, cells/mm^2, median [range]	25.2 [1.9–271.4]	20.9 [0–297.5]	0.363
CD163$^+$CD204$^+$			
Whole, cells/mm^2, median [range]	603.9 [75.5–1990.6]	194.2 [37.3–513.2]	<0.001
Stroma, cells/mm^2, median [range]	1277.2 [304.7–3748.8]	379.9 [81.0–1651.1]	<0.001
Tumor, cells/mm^2, median [range]	545.2 [64.6–1483.7]	123.1 [13.4–462.6]	<0.001
PD-L1 positivity %, median [range]	12.5 [0–94.5]	7.6 [0.2–60.0]	0.040
PD-L1 high cell in CD163$^+$CD204$^+$			
Whole, %, median [range]	10.3 [0–87.6]	2.7 [0–27.9]	<0.001
Stroma, %, median [range]	10.9 [0–89.4]	1.5 [0–29.2]	<0.001
Tumor, %, median [range]	10.1 [0–87.5]	3.9 [0–34.4]	0.004

Note: Clusters 0 and 1 were defined by the *Seurat* package in the R environment.

Abbreviation: PD-L1, programmed cell death ligand 1.

recognized as inflammatory tumors with abundant immune-related cells, whereas cold tumors lack immune-related cells.[34] Similar to hot tumors, cluster 0 formed a population with abundant immune-related cells; TAMs, CD3$^+$, and CD8$^+$ T cells were the main markers in this cluster (Table 4, and Figures 4 and S4). Recently, the combination of atezolizumab (anti-PD-L1 antibody) and bevacizumab (anti-vascular endothelial growth factor antibody) has been approved for unresectable HCC. Anti-PD-L1 antibody binds to the PD-L1 antigen on the surface of both cancerous and TAMs and inhibits the PD-L1/PD-1 and PD-L1/CD80 pathways, resulting in reactivation of anti-tumor immunity by T lymphocytes.[35,36] Therefore, anti-PD-L1 antibody may be effective in patients in cluster 0 with T lymphocytes, TAMs, and TAMs with high PD-L1 expression. In the present study, among the 23 patients with cHCC-CCA, 34.8% of those in C-com and 52.2% of those in H-com were classified into cluster 0, respectively. Similar to the finding of no significant difference between C-com and H-com in the multiple comparisons of immunological characteristics, there was no significant difference in the distribution of the clusters. As expected, cases with high immune cell infiltration in C-com also showed high immune cell infiltration in H-com (Figure 2), and seven

cases (30.4%) were classified as cluster 0, both C-com and H-com. In addition, 34.8% of cases with iCCA were also classified in this cluster, suggesting that components with abundant immune-related cells were also present within iCCA. Contrastingly, since cluster 1 comprised cold tumors with a few lymphocytes, immunotherapies such as adoptive cell transfer of T cells might be proposed.[13,14]

The immunogenicity of tumors is associated with genetic mutations.[37] Mutations in *TP53* and *CTNNB1*, which are common in HCC, and the *IDH1* mutation, which is common in iCCA, are also reported to be associated with the immune microenvironment.[31,38–42] To examine the relationship among TIME analyzed by MFIH and the characteristics of genetic mutations and the transcriptome in tumor tissue, we also collected other cases prospectively. Unfortunately, we have not yet determined key factors to be able to discuss the biological significance of clusters from MFIH using these genetic analyses with this prospective cohort (Figure S5). We believe that this is mainly due to the following reason: it is difficult to stratify the immunological status of each component by genetic analyses with bulk tissue samples, especially in a mixed type of cHCC-iCCA. Immunohistochemistry can be used simultaneously to identify the
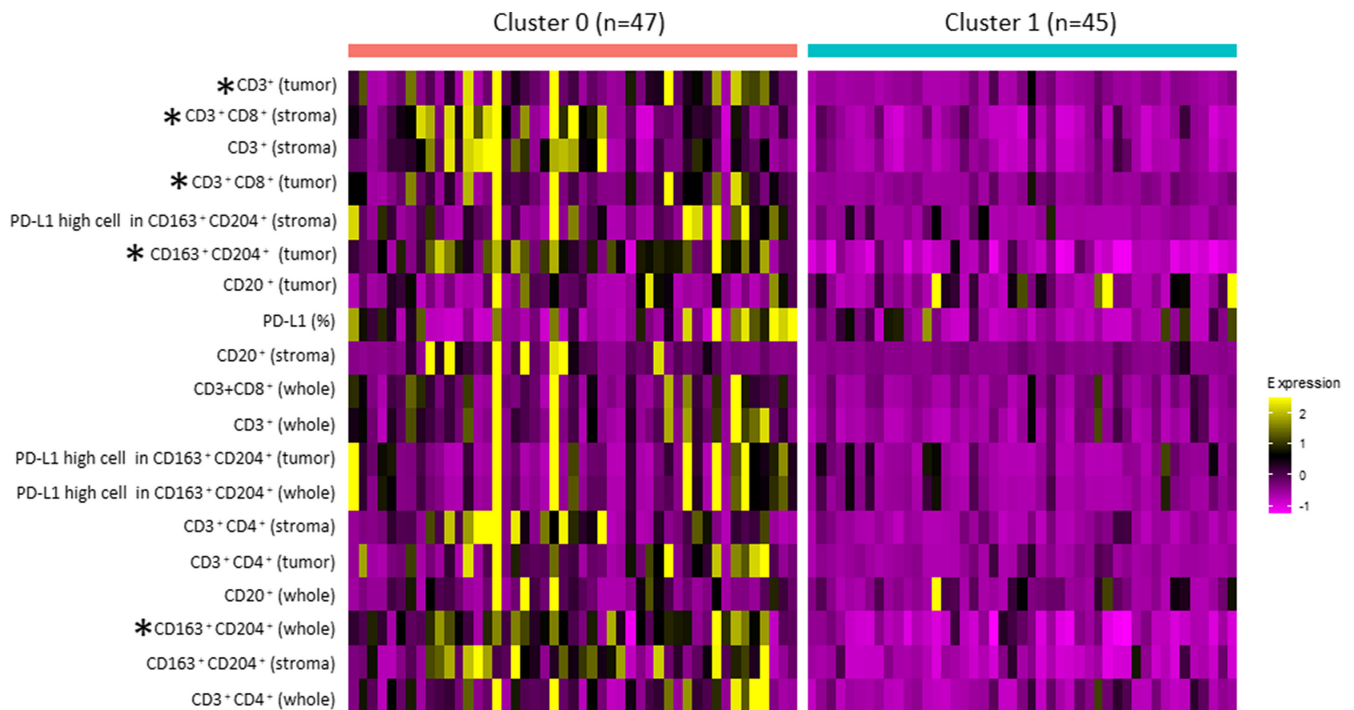
FIGURE 4 Heat map analysis of variables in each patient distributed on clusters 0 and 1. The heat map was created using *Seurat* in R package. Each patient and variable are shown on the horizontal and vertical axes, respectively. Variable expression was normalized and then natural-log transformed using log1p. Asterisks (*) indicate the top five variables contributing to partitioning between clusters

distribution of each immune-related cell based on characteristics such as tissue morphology, tumor markers, tumor, and stromal regions. MFIH also enables the evaluation of multiple markers and assessment of the complex function of immune cells in the same tissue section. We expect that MFIH will facilitate the comprehensive understanding of TIME.

The present study had some limitations. First, the virological status between patients with iCCA and cHCC-CCA could not be matched because almost all the iCCA patients did not have hepatitis virus infections. Considering viral infection is essential information that should be examined in the TIME, we compared TIME between two groups divided based on the presence or absence of viral infection. Although the number of lymphocytes in the virus-infected group was higher than that in the noninfected group, the distributions of the identified clusters did not differ based on the presence or absence of the virus (Figures S6 and S7). It was speculated that the comprehensive evaluation of TIME via cluster analysis using the k-NN parameter with multiple variables from MFIH, including not only lymphocyte infiltration but also PD-L1 expression and TAM activation, identified hot tumors independent of viral infection. Furthermore, accurate prognostic analysis was challenging because the cohort of patients in the present study was small due to the rarity of the disease, and some patients underwent repeat hepatectomy or volume reduction surgery. Although Figure S8 shows that cluster 0 tends to have better prognosis than cluster 1, further studies based on large cohorts at multiple centers, as well as prospective studies, are required to further explore the clinical or research implications of the conclusions of the clustering analysis in the present study.

In conclusion, we could determine the composition of the TIME of cHCC-iCCA using an index for HCC, a carcinoma for which immunotherapy is currently being introduced, and an index of iCCA, a carcinoma for which there are only a few effective immunotherapies. Considering most of the cHCC-iCCA in the present cohort were the mixed type, the boundaries of the tissue regions were very unclear under macroscopy. Approaches such as omics analysis with entire tissue were difficult, therefore we performed an MFIH assay, which is more suitable for the analyzing the TIME of each tissue region clearly. We found no significant differences in immunological features in almost all patients with cHCC-CCA, despite the fact that cHCC-CCA is a heterogeneous tumor comprising C-com and H-com. Comparison of the TIME in C-com and H-com with that in iCCA revealed no significant difference; however, some C-com and H-com cases tended to have more T lymphocytes compared to iCCA. C-com and H-com had fewer TAMs than HCC. Moreover, in cluster analysis based on various immunological features of cHCC-CCA, components with abundant immune-related cells that may be the rationale for immunotherapy indication were identified in cHCC-CCA. Such an approach could facilitate the development of precision medicine for immunotherapy in future.

ORCID

Naoki Yagi https://orcid.org/0000-0002-1299-4423
Toshihiro Suzuki https://orcid.org/0000-0002-7095-6556
Shoichi Mizuno https://orcid.org/0000-0001-6329-6943
Motohiro Kojima https://orcid.org/0000-0002-6150-6545
Masashi Kudo https://orcid.org/0000-0003-2161-1807
Motokazu Sugimoto https://orcid.org/0000-0002-1654-0613
Shin Kobayashi https://orcid.org/0000-0001-9321-8452
Naoto Gotohda https://orcid.org/0000-0002-4468-5844
Genichiro Ishii https://orcid.org/0000-0001-8637-3323
Tetsuya Nakatsura https://orcid.org/0000-0003-3918-2385

REFERENCES

1. Allen RA, Lisa JR. Combined liver cell and bile duct carcinoma. *Am J Pathol*. 1949;25:647-655.
2. Kudo M, Izumi N, Kubo S, et al. Report of the 20th Nationwide follow-up survey of primary liver cancer in Japan. *Hepatol Res*. 2020;50:15-46.
3. Chantajitr S, Wilasrusmee C, Lertsitichai P, Phromsopha N. Combined hepatocellular and cholangiocarcinoma: clinical features and prognostic study in a Thai population. *J Hepatobiliary Pancreat Surg*. 2006;13:537-542.
4. Yin X, Zhang BH, Qiu SJ, et al. Combined hepatocellular carcinoma and cholangiocarcinoma: clinical features, treatment modalities, and prognosis. *Ann Surg Oncol*. 2012;19:2869-2876.
5. Wang AQ, Zheng YC, Du J, et al. Combined hepatocellular cholangiocarcinoma: Controversies to be addressed. *World J Gastroenterol*. 2016;22:4459-4465.
6. Beaufrère A, Calderaro J, Paradis V. Combined hepatocellular-cholangiocarcinoma: An update. *J Hepatol*. 2021;74:1212-1224.
7. Trikalinos NA, Zhou A, Doyle MBM, et al. Systemic therapy for combined hepatocellular-cholangiocarcinoma: a single-institution experience. *J Natl Compr Canc Netw*. 2018;16:1193-1199.
8. Onuma AE, Zhang H, Huang H, Williams TM, Noonan A, Tsung A. Immune checkpoint inhibitors in hepatocellular cancer: current understanding on mechanisms of resistance and biomarkers of response to treatment. *Gene Expr*. 2020;20:53-65.
9. Iwamoto H, Shimose S, Noda Y, et al. Initial experience of atezolizumab plus eevacizumab for unresectable hepatocellular carcinoma in real-World clinical Practice. *Cancers (Basel)*. 2021;13:2786.
10. Finn RS, Qin S, Ikeda M, et al. Atezolizumab plus bevacizumab in unresectable hepatocellular carcinoma. *N Engl J Med*. 2020;382:1894-1905.
11. Taniguchi M, Mizuno S, Yoshikawa T, et al. Peptide vaccine as an adjuvant therapy for glypican-3-positive hepatocellular carcinoma induces peptide-specific CTLs and improves long prognosis. *Cancer Sci*. 2020;111:2747-2759.
12. Sawada Y, Yoshikawa T, Ofuji K, et al. Phase II study of the GPC3-derived peptide vaccine as an adjuvant therapy for hepatocellular carcinoma patients. *Oncoimmunology*. 2016;5:e1129483.
13. Kole C, Charalampakis N, Tsakatikas S, et al. Immunotherapy for hepatocellular carcinoma: a 2021 update. *Cancers (Basel)*. 2020;12(10):2859.
14. Takayama T, Sekine T, Makuuchi M, et al. Adoptive immunotherapy to lower postsurgical recurrence rates of hepatocellular carcinoma: a randomised trial. *Lancet*. 2000;356:802-807.
15. Jakubowski CD, Azad NS. Immune checkpoint inhibitor therapy in biliary tract cancer (cholangiocarcinoma). *Chin Clin Oncol*. 2020;9:2.
16. Ilyas FZ, Beane JD, Pawlik TM. The state of immunotherapy in hepatobiliary cancers. *Cells*. 2021;10.
17. Rizell M, Åberg F, Perman M, et al. Checkpoint inhibition causing complete remission of metastatic combined hepatocellular-cholangiocarcinoma after hepatic resection. *Case Rep Oncol*. 2020;13(1):478-484. Copyright © 2020 by S. Karger AG, Basel.
18. Job S, Rapoud D, Dos Santos A, et al. Identification of four immune subtypes characterized by distinct composition and functions of tumor microenvironment in intrahepatic cholangiocarcinoma. *Hepatology*. 2020;72:965-981.
19. Reck M, Rodríguez-Abreu D, Robinson AG, et al. Pembrolizumab versus chemotherapy for PD-L1-positive non-small-cell lung cancer. *N Engl J Med*. 2016;375:1823-1833.
20. Garon EB, Rizvi NA, Hui R, et al. Pembrolizumab for the treatment of non-small-cell lung cancer. *N Engl J Med*. 2015;372:2018-2028.
21. Chen PL, Roh W, Reuben A, et al. Analysis of immune signatures in longitudinal tumor samples yields insight into biomarkers of response and mechanisms of resistance to immune checkpoint blockade. *Cancer Discov*. 2016;6:827-837.
22. Rashidian M, Ingram JR, Dougan M, et al. Predicting the response to CTLA-4 blockade by longitudinal noninvasive monitoring of CD8 T cells. *J Exp Med*. 2017;214:2243-2255.
23. Tumeh PC, Harview CL, Yearley JH, et al. PD-1 blockade induces responses by inhibiting adaptive immune resistance. *Nature*. 2014;515:568-571.
24. Imaizumi K, Suzuki T, Kojima M, et al. Ki67 expression and localization of T cells after neoadjuvant therapies as reliable predictive markers in rectal cancer. *Cancer Sci*. 2020;111:23-35.
25. Morisue R, Kojima M, Suzuki T, et al. Sarcomatoid hepatocellular carcinoma is distinct from ordinary hepatocellular carcinoma: clinicopathologic, transcriptomic and immunologic analyses. *Int J Cancer*. 2021;149:546-560.
26. Wells HG. Primary carcinoma of the liver. *Am J Med Sci*. 1903;126(3):403-417.
27. Brunt E, Aishima S, Clavien PA, et al. cHCC-CCA: Consensus terminology for primary liver carcinomas with both hepatocytic and cholangiocytic differentiation. *Hepatology*. 2018;68:113-126.
28. Shirakawa H, Kuronuma T, Nishimura Y, et al. Glypican-3 is a useful diagnostic marker for a component of hepatocellular carcinoma in human liver cancer. *Int J Oncol*. 2009;34:649-656.
29. Tsuchiya N, Sawada Y, Endo I, Saito K, Uemura Y, Nakatsura T. Biomarkers for the early diagnosis of hepatocellular carcinoma. *World J Gastroenterol*. 2015;21:10573-10583.
30. Shimizu Y, Suzuki T, Yoshikawa T, et al. Cancer immunotherapy-targeted glypican-3 or neoantigens. *Cancer Sci*. 2018;109:531-541.
31. Zheng BH, Ma JQ, Tian LY, et al. The distribution of immune cells within combined hepatocellular carcinoma and cholangiocarcinoma predicts clinical outcome. *Clin Transl Med*. 2020;10:45-56.
32. Kubota K, Moriyama M, Furukawa S, et al. CD163(+)CD204(+) tumor-associated macrophages contribute to T cell regulation via

interleukin-10 and PD-L1 production in oral squamous cell carcinoma. *Sci Rep.* 2017;7:1755.

33. Hasita H, Komohara Y, Okabe H, et al. Significance of alternatively activated macrophages in patients with intrahepatic cholangiocarcinoma. *Cancer Sci.* 2010;101:1913-1919.

34. Zemek RM, Chin WL, Nowak AK, Millward MJ, Lake RA, Lesterhuis WJ. Sensitizing the tumor microenvironment to immune checkpoint therapy. *Front Immunol.* 2020;11:223.

35. Hui E, Cheung J, Zhu J, et al. T cell costimulatory receptor CD28 is a primary target for PD-1-mediated inhibition. *Science.* 2017;355:1428-1433.

36. Chen DS, Irving BA, Hodi FS. Molecular pathways: next-generation immunotherapy–inhibiting programmed death-ligand 1 and programmed death-1. *Clin Cancer Res.* 2012;18:6580-6587.

37. Rizvi NA, Hellmann MD, Snyder A, et al. Cancer immunology. Mutational landscape determines sensitivity to PD-1 blockade in non-small cell lung cancer. *Science.* 2015;348:124-128.

38. Shi M, Wang Y, Tang W, et al. Identification of TP53 mutation associated-immunotype and prediction of survival in patients with hepatocellular carcinoma. *Ann Transl Med.* 2020;8:321.

39. Xiao X, Mo H, Tu K. CTNNB1 mutation suppresses infiltration of immune cells in hepatocellular carcinoma through miRNA-mediated regulation of chemokine expression. *Int Immunopharmacol.* 2020;89:107043.

40. Kohanbash G, Carrera DA, Shrivastav S, et al. Isocitrate dehydrogenase mutations suppress STAT1 and CD8+ T cell accumulation in gliomas. *J Clin Invest.* 2017;127:1425-1437.

41. Joseph NM, Tsokos CG, Umetsu SE, et al. Genomic profiling of combined hepatocellular-cholangiocarcinoma reveals similar genetics to hepatocellular carcinoma. *J Pathol.* 2019;248:164-178.

42. Liu ZH, Lian BF, Dong QZ, et al. Whole-exome mutational and transcriptional landscapes of combined hepatocellular cholangiocarcinoma and intrahepatic cholangiocarcinoma reveal molecular diversity. *Biochim Biophys Acta Mol Basis Dis.* 2018;1864:2360-2368.

SUPPORTING INFORMATION

Additional supporting information may be found in the online version of the article at the publisher's website.